Non-Linear Filter for Gradient Artefact Correction during Simultaneous EEG-fMRI

José L. Ferreira[*1], Pierre J.M. Cluitmans[2], Ronald M. Aarts[3]

[1,2,3]Department of Electrical Engineering, Eindhoven University of Technology
[2]Kempenhaeghe Epilepsy Center
[3]Philips Research Laboratories Eindhoven
P. O. 513 – 5600 MB – Eindhoven – Netherlands

[*1]j.l.ferreira@tue.nl; [2]p.j.m.cluitmans@tue.nl; [3]r.m.aarts@tue.nl

Abstract

Parallel to the breakthroughs on the usage of simultaneous EEG-fMRI in neurocognitive studies and research, the occurrence of artefacts in the EEG signal induced within the fMRI scanner constitutes one of the challenges to be overcome in order to broaden the range of applications of such a technique. It is the case of the gradient artefact, provoked by the variation of gradient magnetic fields. Thereby, although a number of computational methodologies have yielded a satisfactory correction of the EEG signal, novel approaches have been proposed to improve the quality of the restored EEG. This work presents a novel proposal for modelling the variability of the gradient artefact template estimated during application of the established average artefact subtraction (AAS) method. Implementation of our proposed model and its combination with the AAS method allow an effective elimination of the gradient artefact from EEG recordings. Moreover, our approach performs an adaptive removal of the underlying artefact residuals, according to the signal slope parameter characteristics.

Keywords

Combined EEG-fMRI; Average Artefact Subtraction; Signal Slope Adaption; Non-linear Filtering

Introduction

The usage of simultaneous EEG-fMRI holds a large number of applications in recent years because its powerful capability of providing new insights into the brain function (Villringer et al., 2010). Albeit such a technique was firstly applied in the field of epilepsy (Warach et al., 1996; Seeck et al., 1998), over the years several other neuroscientific studies, research, and applications which make use of the combined EEG-fMRI have been proposed and reported in the literature (Villringer et al., 2010; Ritter and Villringer, 2006).

However, enhancements still remain to be accomplished, regarding the induction of artefacts in the EEG signal by the magnetic fields of the fMRI scanner. In this respect, the quality of the EEG signal acquired during continuous fMRI depends on the performance of hardware solutions as well as computational approaches to minimize and remove the common types of artefacts arising in the electroencephalogram (Allen et al., 1998). That is the case of the so-called "gradient" or "imaging acquisition" artefact (Allen et al., 2000; Mulert and Hegerl, 2009; Ritter et al., 2010).

Gradient artefacts occur in the EEG signal induced by the application of rapidly varying gradient magnetic fields for spatial encoding of the magnetic resonance signal (MR), and radiofrequency pulses (RF) for spin excitation in the circuit formed by the electrodes, leads, patient, and amplifier. They have a waveform which is approximately the differential waveform of the corresponding gradient pulse (Anami et al., 2003; Ritter et al., 2010). The amplitudes of imaging artefacts can be several orders higher than the magnitude of the neuronal EEG signal. According to Ritter et al. (2010), artefacts associated with the gradient switching have amplitude at 10^3 to 10^4 μV, whereas those arising from RF have magnitude up to around 10^2 μV. In turn, the bandwidth of the standard clinical EEG is exceeded by the gradient artefact frequencies, in addition to being overlapped by discrete harmonic artefact frequency intervals, or "frequency bins". As discussed by Niazy et al. (2005), the fundamental of each respective frequency bin corresponds to multiples of the inverse of the EPI slice time parameter.

In order to minimize the induction of gradient artefacts in the EEG signal, a number of hardware solutions have been suggested (Anami et al., 2003; Ritter et al., 2010; Mullinger et al., 2011). Concerning post-processing artefact correction methods, frequency and time-domain techniques have been proposed as

well, like frequency-domain filtering (Hoffmann et al., 2000; Sijbers et al., 1999; Sijbers et al., 2000), average artefact subtraction (AAS) (Allen et al. 2000), principal component analysis (Negishi et al., 2004; Niazy et al., 2005), independent component analysis (Mantini et al., 2007), and spatial filtering (Brookes et al., 2008).

The average artefact subtraction (AAS) is the most established computational methodology for imaging artefact correction. It consists of the calculation of an average artefact waveform (or template) over a fixed number of samples, which is then subtracted from the EEG signal at each sample (Allen et al., 2000). The usage of the AAS method allows a substantial attenuation and removal of the gradient artefact. Nevertheless, as it is assumed that the artefact waveform possesses a constant morphology over the time, and does not take into account its variability, artefact residuals arise in the EEG signal after the template subtraction. Further, effectiveness of the AAS depends on accurate sampling of the gradient artefact waveform and timing-alignment of the fMRI equipment and EEG clocks (Mandelkow et al., 2006; Gonçalves et al., 2007; Freyer et al., 2009). Thereby, additional restoration methods must be carried out in order to achieve a satisfactory signal correction (Allen et al., 2000; Niazy et al., 2005, Gonçalves et al., 2007).

The current work presents a novel approach for modelling and removal of the gradient artefact residuals resulting from application of the AAS method. In this sense, a specific model is proposed to evaluate and quantify the variability of the artefact template waveform. Our approach is modified from Ferreira et al. (2012), and based upon the information of variability contained in the difference between consecutive samples of the digital EEG signal (Cluitmans et al., 1993; Van de Velde et al., 1998; Ferreira et. al, 2013a).

Materials and Methods

Patients

The EEG recordings were collected simultaneously with fMRI data for a research focused on epilepsy and post-traumatic stress disorder (PTSD) (Van Liempt et al., 2011), jointly developed by the department of Psychiatry of Universiteit Medisch Centrum Utrecht, the Research Centre Military Mental Health Care in the Dutch Central Military Hospital in Utrecht, and the Department of Research and Development of the Kempenhaeghe Epilepsy Center in Heeze, The Netherlands.

The data were recorded from military veterans with PTSD which were in mission abroad through the outpatient clinic of the Military Mental Health Care. All participants were male and aged between 18 and 60 years. EEG signal recordings from 15 subjects were used in order to apply and evaluate the methodology we have proposed in this work.

Protocol for Data Acquisition

A 3 T Scanner (Philips, Eindhoven, Netherlands) was employed to carry out the functional magnetic resonance imaging scanning. An MRI-compatible 64 channel polysomnograph was used to collect one ECG channel, two EOG channels, one EMG and 60 EEG channels. The EEG electrodes positioning was in accordance with the $10-20$ international system electrodes placement. The sampling frequency for EEG signal acquiring was 2048 Hz.

Simultaneous EEG-fMRI data were collected during 45 minutes, after application of the EEG cap. The subjects were scanned using a functional echo-planar imaging sequence with 33 transversal slices (thickness 3 mm, TE 30 ms, and TR 2500 ms).

General Overview of the Average Artefact Subtraction Methodology

The basic idea of the average artefact subtraction method consists of estimating an average template of the gradient artefact waveform observed in the raw EEG signal. Such a template is then subtracted from the electroencephalogram at those regions where the artefact occurs (Allen et al., 2000). The average artefact subtraction can be described by Eq. (1) (Ferreira et al., 2012):

$$E\hat{E}G_{corct,i} = EEG_{raw,i} - \Gamma_{i_s} \quad (1)$$

where $\mathbf{E\hat{E}G_{corct}}$ and $\mathbf{EEG_{raw}}$ are, respectively, the corrected EEG after template subtraction and the raw EEG signal; $\mathbf{\Gamma}$ corresponds to the template to be subtracted; i runs over the number of samples within EEG signal; and i_s runs over the template segment.

According to Allen et al. (2000), in order to calculate the template $\mathbf{\Gamma}$, the $\mathbf{EEG_{raw}}$ excerpt is divided into segments of length S. The average of samples situated at the same template position i_s corresponds to the template sample Γ_{i_s}. For continuous fMRI acquisition, S is defined as the EPI slice time parameter (ST). Because of the misalignment between the EEG and fMRI clocks, interpolation and extrapolation within the segments must be performed as well (Allen et al., 2000).

Overview of the Average Artefact Subtraction Methodology Employed in This Work

In this work, the AAS method was also carried out by using the model of Eq. (1). For estimation of the slice time (*ST*), we used the methodology proposed by Garreffa et al. (2003). Observation of the raw data recorded within the MR scanning revealed the occurrence of the typical peaks corresponding to the onset of each MR slice, in such a way that *ST* could be estimated by evaluation of the time interval between two subsequent peaks. For the data under analysis, the value of *ST* was calculated at 155 ± 1 samples, which corresponded to the time interval of 75.68 ± 0.50 ms (Ferreira et al., 2012).

Hence, the raw EEG was divided into segments of 155 samples for estimation of the artefact template. In case of segments which contained more or less than 155 samples, extrapolation or interpolation was done in order to compensate the misalignment between the EEG and fMRI clocks. The number of segments considered for average was 32 slices.

To implement the average artefact subtraction method, we used the approach described in Ferreira et al. (2012).

Modelling of the artefact waveform variability

To identify and remove the remaining residuals resulting from application of the AAS method, a model for quantification of the artefact waveform variability has been proposed, modified from Ferreira et al. (2012). As discussed by these authors, estimation of the template variability could be adaptively implemented by multiplying each artefact template sample by an estimated factor $\hat{a}_i$, and then the subtraction indicated in (1) is performed as follows:

$$E\hat{E}G_{corct,i} = EEG_{raw,i} - \hat{a}_i \Gamma_{i_s} \quad (2)$$

Eq. (2) is, therefore, an adaptive extension of Eq. (1), whose limit referred to as the filter parameter $\hat{a}_i$ allows refining the value of $\mathbf{E\hat{E}G}_{\mathbf{corct}}$ (Klados et al., 2009; Ferreira et al., 2012):

$$\lim_{\hat{a}_i \to a_i} E\hat{E}G_{corct,i} = \text{true} \quad EEG_i \quad (3)$$

in such a way that, as the value of $\hat{a}_i$ is adapted and approximates to the optimal parameter value a_i, the value of $E\hat{E}G_{corct,i}$ would tend to the true EEG_i.

In the current work, **â** was changed to a new parameter **â′**, and Eqs. (2) and (3) have been further modified, resulting in:

$$EEG_{corct,i} = E\hat{E}G_{corct,i} - \hat{a}'_i R_i$$
$$EEG_{corct,i+1} = E\hat{E}G_{corct,i+1} + \hat{a}'_i R_i \quad (4)$$

where the product of the corresponding elements **â′** and **R** acts as an initial estimation of the remaining residual in the $\mathbf{E\hat{E}G}_{\mathbf{corct}}$. Thus, Eq. (4) allows calculating a refinement for the EEG signal corrected by the AAS method. And the respective restored EEG ($\mathbf{EEG}_{\mathbf{corct}}$) is calculated by subtracting the estimation of the remaining residual, $\hat{a}'_i R_i$, from the corresponding unrefined values within $\mathbf{E\hat{E}G}_{\mathbf{corct}}$.

As the product of the corresponding elements of **â′** and **R** should model the variability of the gradient artefact, for their estimation we have sought and taken into account specific properties of the raw EEG, the EEG corrected by AAS, and the true EEG signal which could reflect such a variability. In this way, the signal slope parameter was assumed to possess such characteristics.

The analysis of the signal slope represented by the difference between consecutive samples can be employed to detect high-frequency properties and artefacts in digital signals (Barlow, 1983; Cluitmans et al., 1993; Van de Velde et al., 1998; Ferreira et al., 2012). The use of the signal slope is in accordance with Cluitmans et al. (1993) and Van de Velde et al. (1998) who described such a signal parameter associated with the large signal magnitudes as being particularly useful for detection of the high-frequency properties of the muscle artefact. In the same way, observation of the EEG recorded within the fMRI scanner reveals that large slopes and magnitudes of the signal can be attributed to the gradient artefact and its residuals as well (Koskinen and Vartiainen, 2009; Ferreira et al., 2012). Thus, the slope variation was also employed to identify the imaging acquisition artefact, described as follows.

According to Ferreira et al. (2012), the larger slopes related to the sharp wave activity of the gradient artefact residuals are used to identify whether the EEG samples are artefact-free or not. In order to perform this identification, a slope threshold (*thrs*) is estimated in such a way that if the sample has signal slope larger than *thrs*, it is then identified containing artefact interference. *thrs* can be estimated, for example, considering the probability distribution of the signal slope (Cluitmans et al., 1993; Van de Velde et al., 1998).

In this way, we have taken into account the probability distributions of an artefact free EEG ($\mathbf{EEG}_{\mathbf{true}}$) and the

$\mathbf{E\hat{E}G}_{corct}$ excerpts, both ones picked up from the same EEG channel of one specific subject. The true EEG was obtained from a raw EEG interval recorded within the scanner with no gradient magnetic field variation. It was observed that more than 90% of the values for the signal slope of the $\mathbf{E\hat{E}G}_{corct}$, *diff* ($\mathbf{E\hat{E}G}_{corct}$), are above the threshold calculated using the $\mathbf{EEG}_{true}$ excerpt (Ferreira et al., 2013b):

$$thrs = \mu_{diff(\mathrm{EEG_{true}})} + 3\sigma_{diff(\mathrm{EEG_{true}})} \quad (5)$$

Furthermore, the probability distribution of the slope parameter estimated for the true EEG ($\mathbf{EEG}_{true}$) closely resembles Gaussian distributions (Cluitmans et al., 1993), in such a way that the confidence interval associated with $\mu_{diff(\mathbf{EEG}_{true})} + 3\sigma_{diff(\mathbf{EEG}_{true})}$ encompasses approximately 99.5% of the distribution (Papoulis and Pillai, 2002). Thus, estimation of *thrs* was performed by using Eq. (5).

The maximum absolute value of the difference between consecutive samples of the signal $\mathbf{E\hat{E}G}_{corct}$ corresponds to the parameter r_i which is related to *diff* ($\mathbf{E\hat{E}G}_{corct}$) by the following expression (Ferreira et al., 2013a):

$$r_i = \max\left|diff(\mathrm{E\hat{E}G_{corct}})\right| \quad (6)$$

where i is the subscript of the maximum slope within *diff* ($\mathbf{E\hat{E}G}_{corct}$).

The two consecutive samples $E\hat{E}G_{corct,i}$ and $E\hat{E}G_{corct,i+1}$ associated with r_i are adapted as follows:

$$EEG_{corct,i} = E\hat{E}G_{corct,i} - L_i$$
$$EEG_{corct,i+1} = E\hat{E}G_{corct,i+1} + L_i \quad (7)$$

where

$$L_i = p \times r_i \quad (8)$$

p is the adaption factor $(0 < p < 1)$ to be applied to the parameter r_i. We experimentally determined and set the value of p as 0.925 (Ferreira et al. 2013b). Therefore, the product $\hat{a}_i' R_i$ of Eq. (4) corresponds to L_i in Eq. (8). In Eq. (7), the sign of L_i is set positive when $E\hat{E}G_{corct,i} > E\hat{E}G_{corct,i+1}$, and vice-versa. The signal $\mathbf{E\hat{E}G}_{corct}$ in equation (6) is then replaced by the modified signal $\mathbf{EEG}_{corct}$, which contains the adapted samples $EEG_{corct,i}$ and $EEG_{corct,i+1}$. Eqs. (6), (7), and (8) are iteratively recalculated until $r_i \le thrs$ (Ferreira et al. 2013b).

According to our approach, therefore, in addition to acting as an indicator of the presence of the gradient artefact residuals in the $\mathbf{E\hat{E}G}_{corct}$ (Cluitmans et al., 1993; Van de Velde et al., 1998), the signal slope parameter, *diff* ($\mathbf{E\hat{E}G}_{corct}$), is also used to estimate the amount of correctness (within L_i) associated with the template variability, to be applied and restore the signal $E\hat{E}G_{corct,i}$ (Ferreira et al., 2012). Thereby, removal of the artefact is performed in an adaptive way by approximating the value of the parameter r_i to the slope characteristics of the raw EEG, corresponding to the threshold *thrs*.

In comparison to the method presented in Ferreira et al. (2012), the usage of Eqs. (5) – (8) shows itself to be more robust and effective on removing stronger gradient artefact interference. Although both approaches make use of the information of variability contained in the signal slope parameter, the former is based upon normalized values of the signal slope parameter, whereas according to the latter, the magnitude of the difference between consecutive samples is used instead (Eq. 6). Moreover, in this work we did not take into account the standard deviation associated to the template average for modelling the variability of the residuals. It was noticed that estimation of such variability is more accurate as performed by Eqs. (5) – (8).

Validation

A set of validation EEG channels, FP1, F3, F8, T5, P3, Oz, CP1, FC5, AFz, F6, C2, TP7, CP4, and POz, was used for evaluation of the proposed model for the artefact residuals from the AAS method and respective EEG restoration. In this sense, the median attenuation of the power spectrum associated with the artefact frequency bins (Niazy et al., 2005) as well as within the range of the clinical EEG (0 – 24 Hz) was assessed. Comparison with the signal restoration achieved by the usage of a linear low-pass filter was also performed.

Results

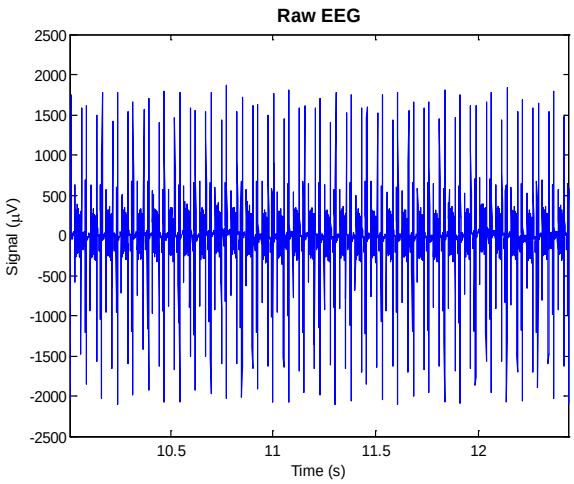

FIG. 1 REPRESENTATIVE RAW EEG SELECTED FOR ILUSTRATION OF APPLICATION OF OUR PROPOSED METHODOLOGY

Fig. 1 depicts a typical EEG excerpt containing strong artefact interference (at 3.7 mV pk-pk), selected from

the recordings of one subject, electrode position F6. The steep wave activity associated with the gradient artefact can be observed in the EEG signal, which is completely obscured by the gradient artefact. Such an EEG excerpt was segmented as well as interpolated or extrapolated depending on the need, according to the AAS method (Allen et al. 2000). The set of 32 slices used for template averaging is shown in Fig. 2.

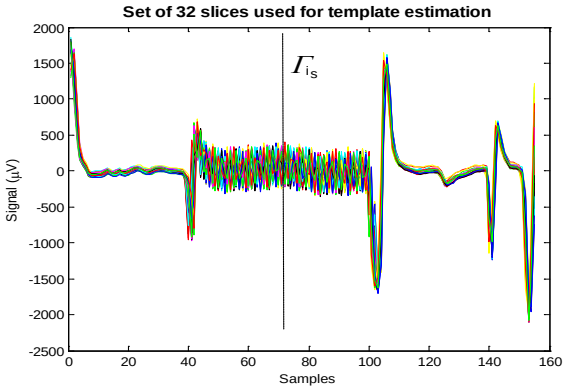

FIG. 2 SET OF 32 SUBSEQUENT SEGMENTS (32 SLICES) IN WHICH THE SIGNAL OF FIG. 1 WAS DIVIDED FOR ARTEFACT TEMPLATE ESTIMATION (155 SAMPLES)

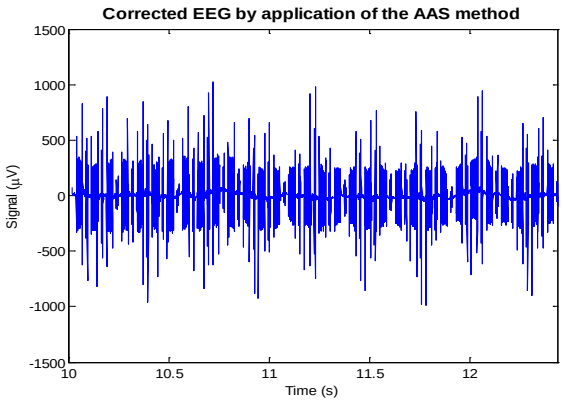

FIG. 3 CORRECTED EEG SIGNAL ($\mathbf{E\hat{E}G}_{corct}$), RESULTING FROM THE APPLICATION OF THE AAS METHOD

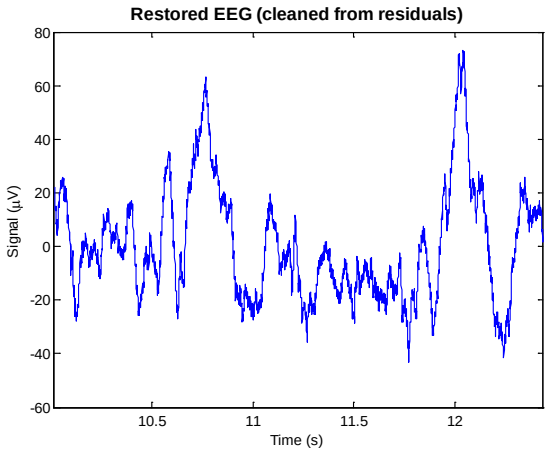

FIG. 4 RESTORED EEG SIGNAL ($\mathbf{EEG}_{corct}$), RESULTING FROM THE APPLICATION OF EQS. (5) – (8) IN THE SIGNAL $\mathbf{E\hat{E}G}_{corct}$ DEPICTED IN FIG. 3

Fig. 3 shows the signal $\mathbf{E\hat{E}G}_{corct}$ resulting from the application of the average artefact subtraction methodology in the raw EEG signal depicted in Fig. 1. A considerable amount of residual artefact remained in the $\mathbf{E\hat{E}G}_{corct}$ after the template subtraction (at 2.0 mV pk-pk). It can be attributed to the large amplitudes and variability of the artefact waveform over the time, as observed in Fig. 2 for the segmented EEG slices. Hence, in order to restore the EEG signal, the model described by Eqs. (5) – (8) was then applied to the signal $\mathbf{E\hat{E}G}_{corct}$ of Fig. 3. The resulting $\mathbf{EEG}_{corct}$ is depicted in Fig. 4. From this figure, it can be observed that the artefact residuals were strongly cleaned up.

As shown in Figs. 5 and 6, our approach removes high-frequency artefact residuals components, as it is performed by a low-pass filter. A linear low-pass filter was used for comparison purposes, set up as a 55-coefficients FIR, cut-off frequency 70 Hz. Moreover, our approach also causes an adaptive attenuation of underlying artefact residuals components within the EEG bandwidth, which can be noticed in Fig. 6d.

According to Niazy et al. (2005) underlying gradient artefact components arise and leak into the frequency bins intervals, region of ±1 Hz around the multiples of the inverse of *ST*. The linear low-pass filter does not yield effective elimination of frequencies below the filter cut-off frequency and, therefore, it also does not attenuate the respective underlying artefact residuals in the EEG bandwidth, as depicted in Fig. 5b (short peaks approximately even spaced) and Fig. 6b. On the other hand, low-frequency artefact components are attenuated by application of our approach in such a way that those residuals have been cleaned up in the restored EEG signal of Fig 5a.

In Table 1, the median spectral power attenuation provoked by application of our approach and the linear filter is shown. The attenuation was calculated using Eq. (9):

$$\text{Attenuation} = 100 \times \text{absolute}\left(\frac{S_{AAS}-S_R}{S_{AAS}}\right)\% \qquad (9)$$

where S_{AAS} is the power spectrum of the EEG corrected by the AAS method; and S_R is the power spectrum of the restored EEG. Regarding the EEG validation channels, the median spectral power attenuation within the frequency bins 13.2, 26.4, 39.6, 52.9, 66.1, 79.3, and 92.5 Hz achieved by the application of our approach is higher than that provoked by the linear filter for frequencies below the filter cut-off frequency. It even can be noticed that application of the filter amplifies the energy of some frequency bins. Our approach has caused higher power attenuation in the

ranges 4 – 8 (6.6%) and 8 – 12 Hz (17%) as well. The median value of the remaining artefact in the restored EEG after application of Eqs. (5) – (8) was 2.9 μV pk-pk.

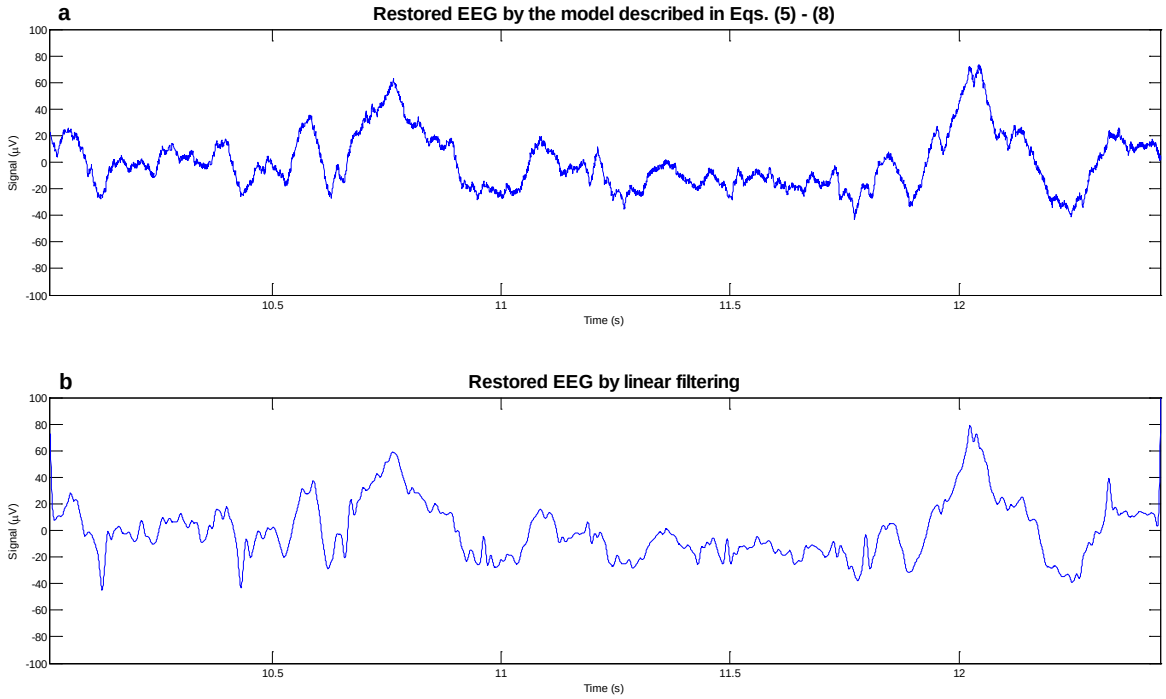

FIG. 5 EEG RESTORATION ASSOCIATED WITH THE SIGNAL $\hat{\mathbf{EEG}}_{\mathbf{coret}}$ DEPICTED IN FIG. 3, OBTAINED BY (A) THE PROPOSED MODEL FOR ARTEFACT RESIDUALS DESCRIBED IN EQS. (5) – (8), AND BY (B) A LINEAR LOW-PASS FILTER

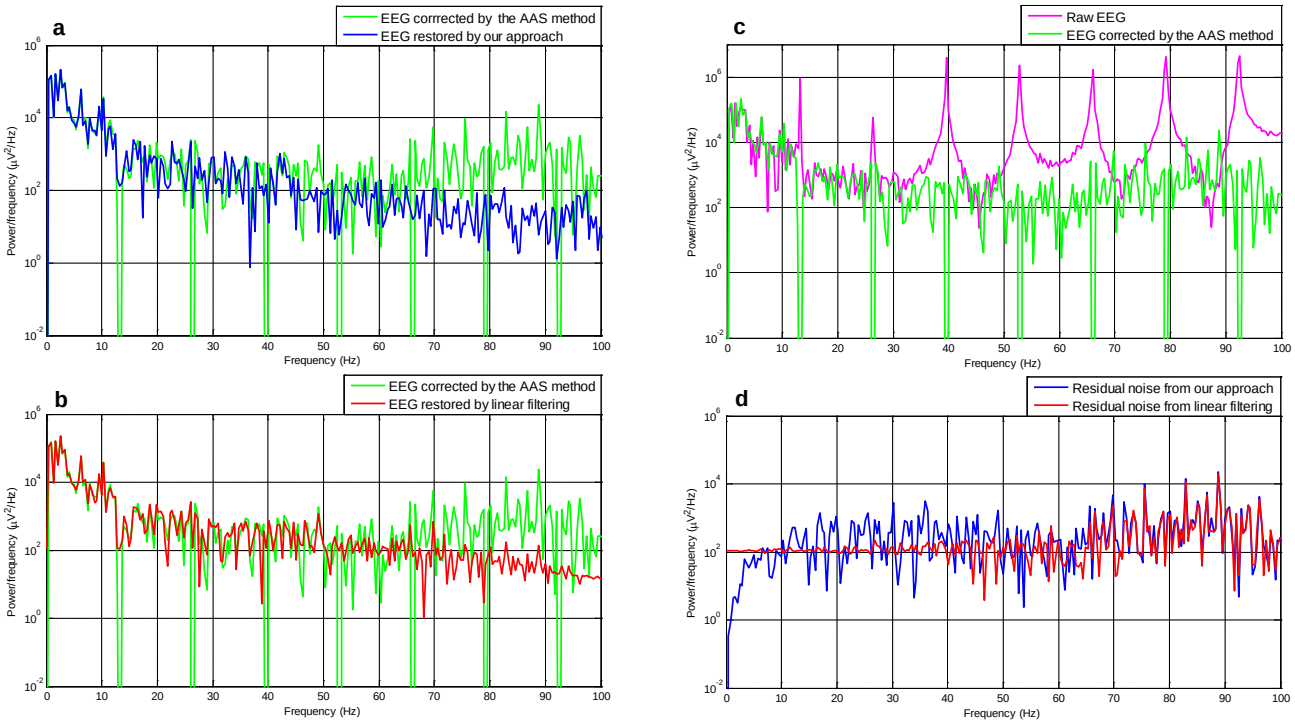

FIG. 6 COMPARISON BETWEEN THE POWER SPECTRUM OF THE EEG CORRECTED BY THE AAS METHOD (FIG. 3) AND: (A) THE POWER SPECTRUM OF THE EEG RESTORED BY OUR APPROACH (FIG. 5A); (B) THE POWER SPECTRUM OF THE EEG RESTORED BY LINEAR FILTERING (FIG. 5B); AND (C) THE POWER SPECTRUM OF THE RAW EEG SIGNAL (FIG. 1). (D) POWER SPECTRUM OF THE RESIDUAL NOISE RESULTING FROM APPLICATION OF OUR APROACH AND LINEAR FILTERING IN THE SIGNAL OF FIG. 3

TABLE 1 MEDIAN SPECTRAL POWER ATTENUATION PROVOKED BY APPLICATION OF OUR APPROACH AND LINEAR FILTERING AFTER AVERAGE TEMPLATE SUBTRACTION, CONSIDERING THE EEG VALIDATION CHANNELS

Restoration Method	Attenuation (%)										
	EEG Frequency Bands (Hz)				Artefact Frequency Bins (Hz)						
	0 – 4	4 – 8	8 – 12	12 – 24	13.2	26.4	39.6	52.9	66.1	79.3	92.5
Our approach	1,1	6,6	17,0	34,7	28,6	56,4	72,9	83,6	87,9	94,8	96,1
Linear filtering	2,7	4,9	6,7	37,7	26,5	184,2	297,3	228,6	264,2	98,2	93,4

Discussion

Application of the average artefact subtraction method allows substantial removal of gradient artefact components. However, partial failure of such a method occurs because the variability of the gradient artefact waveform over the time, as can be observed in Fig. 3. Thereby, the usage of further correction approaches is required for removal of the artefact residuals (Allen et al., 2000; Niazy et al., 2005).

High-frequency artefact residuals which exceed the range of the clinical EEG can be promptly cleaned up by applying linear low-pass filters, as depicted in Figs. 5b and 6b. However, the underlying residuals within the EEG bandwidth are not removed by linear filtering, demanding further correction techniques (Allen et al., 2000). In this respect, we have proposed the model of Eqs. (5) – (8) to quantify and remove the remaining artefact residuals. Such a model constitutes a non-linear filter approach based on the signal slope parameter, which attempts to minimize the variability over the time associated with the estimated artefact template.

In addition to eliminating the high-frequency artefact residuals components, our approach performs an adaptive attenuation of the underlying artefact residuals, as depicted in Figs. 4, 5, and 6, and observed in Table 1. Unlike a linear low-pass filter, our proposed model adapts only the samples of the signal which have signal slope higher than *thrs* (Ferreira et al., 2013a). Hence, the other samples are not adapted and, in consequence, are not distorted by the filtering process. This fact explains the lower signal distortion provoked with the application of our approach. Further, as the model described in Eqs. (5) – (8) takes into account a specific property of the artefact (i.e., the signal slope parameter), it attenuates the residuals in accordance with the artefact slope characteristics. Thereby, application of Eqs. (5) – (8) in the signal $\mathbf{\hat{EEG}}_{corct}$ adapts *firstly* the signal slope parameter associated with the underlying artefact residuals, which are larger than that of the clinical EEG. Therefore, artefact residuals and eventual leakage around the corresponding frequency bins (Niazy et al., 2005) are attenuated without a preliminary need for using additional correction techniques.

It is noteworthy that our methodology is even effective within a strong artefact interference scenario, as depicted in Fig. 1, whereas the method presented in Ferreira et al. (2012) is suitable to remove artefact residuals with lower order magnitudes (at 150 μV pk-pk). To smooth the restored EEG signal, a moving-average filter could be used as well after application of Eqs. (5) – (8) (Ferreira et al., 2013b). In future work, further improvements concerning the computational performance of such a non-linear filter shall be done. Also, our methodology shall be assessed for gradient artefacts induced in the EEG signal within other types of fMRI scanners. Finally, the proposed approach shall be evaluated for digital filtering and correction of other types of artefact as well.

Conclusions

In this work, a non-linear filter approach is proposed for modelling of the gradient artefact residuals resulting from application of the established AAS method.

Implementation of our approach is based upon the idea of minimizing the variability associated with the artefact template waveform. In this respect, the signal slope parameter, defined as the difference between consecutive samples of the digital EEG signal, is employed to estimate such variability.

The proposed model performs an adaptive artefact filtering of high-frequency artefact residuals components as well as underlying components in the EEG bandwidth. Therefore, combination of our modelling approach with the AAS method allows effective artefact residuals attenuation and EEG restoration. Hence, our method could be used and even combined with other artefact correction techniques in order to improve the quality of the EEG signal acquired within the fMRI scanner.

ACKNOWLEDGMENT

We are grateful to Saskia van Liempt, M.D., and Col. Eric Vermetten, M.D., Ph.D. from the University Medical Center/Central Military Hospital, Utrecht, for providing the data presented in this work. This work has been made possible by a grant from the European Union and Erasmus Mundus – EBW II Project, and by a grant from CNPq – Science without Borders Program.

REFERENCES

Allen, P., Polizzi, G., Krakow, K., Fish, D., Lemieux, L. "Identification of EEG events in the MR scanner: the problem of pulse artefact and a method for its subtraction." NeuroImage 8 (1998): 229-239.

Allen, P., Josephs, O., Turner, R. "A method for removing imaging artifact from continuous EEG recorded during functional MRI." NeuroImage 12 (2000): 230-239.

Anami, K. et al. "Stepping stone sampling for retrieving artifact-free electroencephalogram during functional magnetic resonance imaging." NeuroImage 19 (2003): 281–295.

Barlow, J. "Muscle spike artifact minimization in EEGs by time-domain filtering." Electroencephalogr. Clin. Neurophysiol. 55 (1983): 487-491.

Brookes, M., Mullinger, K., Stevenson, C., Morris, P., Bowtell, R. "Simultaneous EEG source localisation and artefact rejection during concurrent fMRI by means of spatial filtering." NeuroImage 40 (2008): 1090-1104.

Cluitmans, P., Jansen, J., Beneken, J. "Artefact detection and removal during auditory evoked potential monitoring." J. Clin. Monit. 9 (1993): 112–120.

Ferreira, J., Cluitmans, P., Aarts, R.M. "Gradient artefact correction in the EEG signal recorded within the fMRI scanner." 5th International Conference on Bio-inspired Systems and Signal Processing, BIOSIGNALS 2012, Vilamoura, Portugal, February 1-4, 2012, Proceedings: 110-117, 2012.

Ferreira, J., Cluitmans, P., Aarts, R.M. "Detection of sharp wave activity in biological signals using differentiation between consecutive samples." 6th International Conference on Bio-inspired Systems and Signal Processing, BIOSIGNALS 2013, Barcelona, Spain, February 11-14, 2013a, Proceedings: 327-332, 2013.

Ferreira, J., Cluitmans, P., Aarts, R.M. "Gradient artefact modelling using a set of sinusoidal waveforms for EEG correction during continuous fMRI." Signal Processing Research 2 (2013b): 39-48.

Freyer, F., Becker, R., Anami, K., Curio, G., Villringer, A., Ritter, P. "Ultrahigh-frequency EEG during fMRI: pushing the limits of imaging-artifact correction." NeuroImage 48 (2009): 94-108.

Garreffa, G. et. al. "Real-time MR artifacts filtering during continuous EEG/fMRI acquisition." Magn. Res. Imaging. 21 (2003): 1175-1189.

Gonçalves, S., Pouwels, P., Kuijer, J., Heethaar, R., de Munck, J. "Artifact removal in co-registered EEG/fMRI by selective average subtraction." Clin. Neurophysiol. 118 (2007): 823-838.

Hoffmann, A., Jäger, L., Werhahn, K., Jaschke, M., Noachtar, S., Reiser, M. "Electroencephalography during functional echo-planar imaging: detection of epileptic spikes using post-processing methods." Magn. Res. Med. 44 (2000): 791-798.

Klados, M., Papadelis, C., Bamidis, P. "A new hybrid method for EOG artifact rejection." 9th International Conference on Information Technology and Application in Biomedicine, ITAB 2009, Larnaca, Cyprus, November 5-7, 2009, Proceedings: 4937-4940, 2009.

Koskinen, M., Vartiainen, N. "Removal of imaging artifacts in EEG during simultaneous EEG/fMRI recording: reconstruction of a high-precision artifact template." NeuroImage 46 (2009): 160-167.

Mandelkow, H., Halder, P., Boesiger, P., Brandeis, D. "Synchronization facilitates removal of MRI artefacts from concurrent EEG recordings and increases usable bandwidth." NeuroImage 32 (2006): 1120-1126.

Mantini, D., Perucci, M., Cugini, S., Romani, G., Del Gratta, C. "Complete artifact removal for EEG recorded during continuous fMRI using independent component analysis." NeuroImage 34 (2007) 598-607.

Mulert, C., Hegerl, U. "Integration of EEG and fMRI." In Neural correlation of thinking, edited by E. Kraft, G. Gulyás, E. Pöppel, 95-106. Verlag, Berlin, Heidelberg: Springer, 2009.

Mullinger, K., Yan, W., Bowtell, R. "Reducing the gradient artefact in simultaneous EEG-fMRI by adjusting the subject's axial position." NeuroImage 54 (2011): 1942-1950.

Negishi, M., Abildgaard, M., Nixon, T., Constable, R. "Removal of time-varying gradient artifacts during continuous fMRI." Clin. Neurophysiol. 115 (2004): 2181-2192.

Niazy, R., Beckmann, C., Iannetti, G., Brady, J., Smith S. "Removal of FMRI environment artifacts from EEG data using optimal basis sets." NeuroImage 28 (2005): 720-737.

Papoulis, A.; Pillai, S. Probability, random variables, and stochastic processes. 4th ed. New York: McGraw-Hill, 2002.

Ritter, P., Becker, R., Freyer, F., Villringer, A. "EEG quality: the image acquisition artifact." In EEG-fMRI: Physiological basis, technique and applications, edited by C. Mulert, L. Limieux, 153-171. Verlag, Berlin, Heidelberg: Springer, 2010.

Ritter, P., Villringer, A. "Simultaneous EEG-fMRI." Neurosci. Biobehav. Rev. 30 (2006): 823-838.

Seeck, M. et al. "Non-invasive epileptic focus localization using EEG-triggered functional MRI and electromagnetic tomography." Electroencephalogr. Clin. Neurophysiol. 106 (1998): 508-512.

Sijbers, J., Michiels, I., Verhoye, M., van Auderkerke, J., van der Linden, A., van Dyck, D. "Restoration of MR-induced artifacts in simultaneously recorded MR/EEG data." Magn. Res. Imaging. 17(1999): 1383-1391.

Sijbers, J., van Audekerke, J., Verhoye, M., van der Linden, A., van Dyck, D. "Reduction of ECG and gradient related artifacts in simultaneously recorded human EEG/fMRI data." Magn. Reson. Imaging. 18 (2000): 881-886.

Van de Velde, M., Van Erp, G., Cluitmans, P. "Detection of muscle artefact in the normal human awake EEG." Electroencephalogr. Clin. Neurophysiol. 107 (1998): 149-158.

Van Liempt, S., Vermetten, E., Lentjes, E., Arends, J., Westenberg, H. "Decreased nocturnal growth hormone secretion and sleep fragmentation in combat-related posttraumatic stress disorder; potential predictors of impaired memory consolidation." Psychoneuroendocrino. 36 (2011): 1361-1369.

Villringer, A., Mulert, C., Lemieux, L. "Principles of multimodal functional imaging and data integration." In EEG-fMRI: Physiological basis, technique and applications, edited by C. Mulert, L. Limieux, 3-17. Verlag, Berlin, Heidelberg: Springer, 2010.

Warach, S., Ives, J., Schlaug, G., Patel, M., Darby, D., Thangaraj, V., Edelman, R., Schomer, D. "EEG-triggered echo-planar functional MRI in epilepsy." Neurology 47 (1996): 89-93.